Tunable, femtosecond pulse source operating in the range 1.06–1.33 μm based on an Yb^{3+}-doped holey fiber amplifier

J. H. V. Price, K. Furusawa, T. M. Monro, L. Lefort, and D. J. Richardson

Optoelectronics Research Centre, University of Southampton, Southampton SO17 1BJ, UK

Received September 10, 2001

We report soliton pulse formation and amplification and soliton-self-frequency shifting in an anomalously dispersive, Yb^{3+}-doped holey fiber amplifier seeded with pulses from an Yb^{3+}-doped, 1.06-μm fiber based mode-locked oscillator. Our fiber-based system provides a highly practical, all-diode-pumped, continuously tunable femtosecond pulse source operational in the important and difficult to reach wavelength range from 1.06 to 1.33 μm. In other experiments multipulse, multicolored soliton formation was observed with wavelength-shifted pulsed output to beyond 1.58 μm. Supercontinuum generation and nonlinear compression of pulses to 65 fs were also obtained with other configurations. © 2002 Optical Society of America

OCIS codes: 060.2320, 060.4370, 190.2640, 190.5650, 999.9999.

1. INTRODUCTION

Wavelength tunable femtosecond optical pulse sources have applications in areas as diverse as ultrafast spectroscopy, materials processing, optoelectronics, nonlinear optics, and optical chemistry. Traditionally, femtosecond pulse sources have been based on bulk crystal materials (most commonly Ti:sapphire) and have employed passive mode-locking techniques, such as Kerr-lens mode locking, that make use of fast intracavity saturable-absorber effects. Whereas excellent performance characteristics have been achieved, and successful commercial products and application areas have been developed, these traditional sources offer a limited range of directly accessible wavelengths and continuous broadband tuning ranges, particularly above 1.1 μm. In general, extending this femtosecond technology to obtain broader tuning ranges and longer wavelengths requires the use of bulk parametric nonlinear devices such as optical parametric oscillators, generators, or amplifiers pumped by bulk femtosecond lasers. Such devices add to the complexity and cost and increase the physical size of the overall system. Moreover, bulk crystal lasers require high-precision alignment and are often pumped by expensive, high-maintenance gas lasers.

The discovery of the soliton-self-frequency shift (SSFS) in optical fibers was reported in 1985–1986,[1–3] and led to the exciting possibility of obtaining widely wavelength tunable femtosecond soliton pulses from fiber-based sources (ideally incorporating a fiber-based pump laser).[4] Indeed, the SSFS in silica fiber was recently used to produce tunable femtosecond pulses over the wavelength range 1.55–2.2 μm in a commercial system incorporating a compact, mode-locked erbium fiber laser as the pump source.[5] This system, with an additional frequency-doubling stage, is now marketed as a compact 1.06-μm laser system.

For the SSFS effect to be obtained the frequency-shifting fiber must exhibit anomalous dispersion both at the initial seed wavelength and across the required tuning range. With conventional single-mode fiber technology it is possible to obtain anomalous dispersion only for wavelengths beyond ~1.3 μm, which precludes the use of SSFS in conjunction with Yb^{3+}-based fiber lasers operating near 1 μm. However, it was shown recently that it is possible to obtain anomalous dispersion at wavelengths that extend into the visible regions of the spectrum by exploiting the unusual properties of small-core holey fibers[6] (or, less practically, by using tapered standard fibers with similarly small core dimensions[7]). These holey (microstructured) fibers are of great practical interest because the incorporation of air holes to define the cladding region allows for a larger range of fiber parameters than for conventional fiber. In particular, the large refractive-index difference between air and glass leads to a range of unique dispersion and nonlinear properties. As an example, the dispersion of a holey fiber has been shown to be particularly sensitive to the hole arrangement, and a wide range of dispersion properties has been demonstrated, including anomalous dispersion down to visible wavelengths, broadband flattened dispersion,[8] and large normal dispersion.[9] One can also tailor the effective mode area in a holey fiber by as much as 3 orders of magnitude by altering the scale of the transverse refractive index profile,[8] leading to fibers with either high or low optical nonlinearities as required for a wide variety of applications.

A holey fiber fabricated to have anomalous dispersion at wavelengths below 1.3 μm must have a small core (typically <2.5 μm in diameter) and a high air fill fraction in the cladding. These properties produce a strong (anomalous) waveguide contribution to the dispersion to compensate for the (normal) material disperision of silica at these wavelengths. The small core naturally leads to the fiber's having an exceptionally high effective nonlinearity, which is ideal for soliton generation. Soliton generation in a small-core holey fiber has already been dem-

onstrated at visible wavelengths, and SSFS wavelength tuning from 1.3–1.6 μm has been demonstrated with tapered microstructured fiber.[10] For these high-nonlinearity holey fibers, just picojoule pulse energies (~200-W typical peak power) and meter-long fiber lengths are required for formation of solitons[6,11,12]; such power levels and fiber lengths are at least an order of magnitude lower than those required for similar experiments with conventional fiber types.[13] We mention also that holey fibers have been demonstrated to provide an ideal medium for supercontinuum generation, which, because of the frequency comb incorporated within the spectrum, is providing great advances in metrology.[14]

In this paper we report what we believe is the first demonstration of a continuously tunable soliton source that operates in the wavelength range 1.06–1.33 μm and is based on holey fiber technology. The system comprises an Yb^{3+}-doped holey fiber amplifier seeded with pulses from an Yb^{3+}-doped, 1.06-μm fiber based mode-locked oscillator. The 1.0–1.3-μm wavelength range is of practical significance; for example, a 1.24-μm source is optimal for many three-photon microscopy applications. However, ultrafast pulses in this wavelength range are difficult to access by conventional means except, as mentioned above, through the use of research grade optical parametric oscillators.

Our new source, based on a diode-pumped Yb^{3+}-doped silica fiber seed laser, relies on SSFS effects in a holey fiber amplifier, which has anomalous dispersion across an extended wavelength range. Use of an amplifying holey fiber to provide the wavelength shifting differs in several aspects to use of the anomalously dispersive passive fiber as demonstrated in other wavelength regimes. First, it allows us to wavelength shift relatively low-energy seed pulses directly from a simple diode-pumped fiber oscillator (previous demonstrations have used substantially higher energy seed pulses, typically of the order of 1 nJ). Second, it allows us to control the wavelength of the output pulses by changing amplifier pump power. Finally, the distributed amplification process enables us to tune over a broader frequency range than has hitherto been possible with passive devices; with our current system we could obtain femtosecond pulses at wavelengths as long as 1.58 μm, corresponding to a frequency shift of 69 THz, which is one third of the frequency of the input pulses.

This paper is structured as follows: In Section 2 we describe the physical operating principles of the system and give details of how the system was implemented and the properties of the holey fiber. In Section 3 we describe and discuss the results of our experiment, and in Section 4 we draw our conclusions.

2. SYSTEM OPERATING PRINCIPLES AND IMPLEMENTATION

As mentioned in Section 1, our source comprises an Yb^{3+}-doped fiber seed laser and an Yb^{3+}-doped holey fiber amplifier. A schematic of the system is shown in Fig. 1. The mode-locked laser produces ultrashort pulses with a positive linear chirp at a wavelength of 1.06 μm. The pulses are launched into the anomalously dispersive, Yb^{3+}-doped holey fiber amplifier, together with a separate pump beam (diode laser) that controls the gain. As a result of the amplification and nonlinear pulse evolution of the pulses as they pass through the amplifier, Raman solitons form and are continuously wavelength shifted through the SSFS. The nonlinear evolution of the pulses depends critically on the pulse peak power, so one tunes the wavelength of the Raman solitons at the amplifier output by varying the gain in the amplifier (controlled by the pump laser). In this way, monocolor soliton output pulses have been wavelength tuned throughout the 1.06–1.33-μm range.

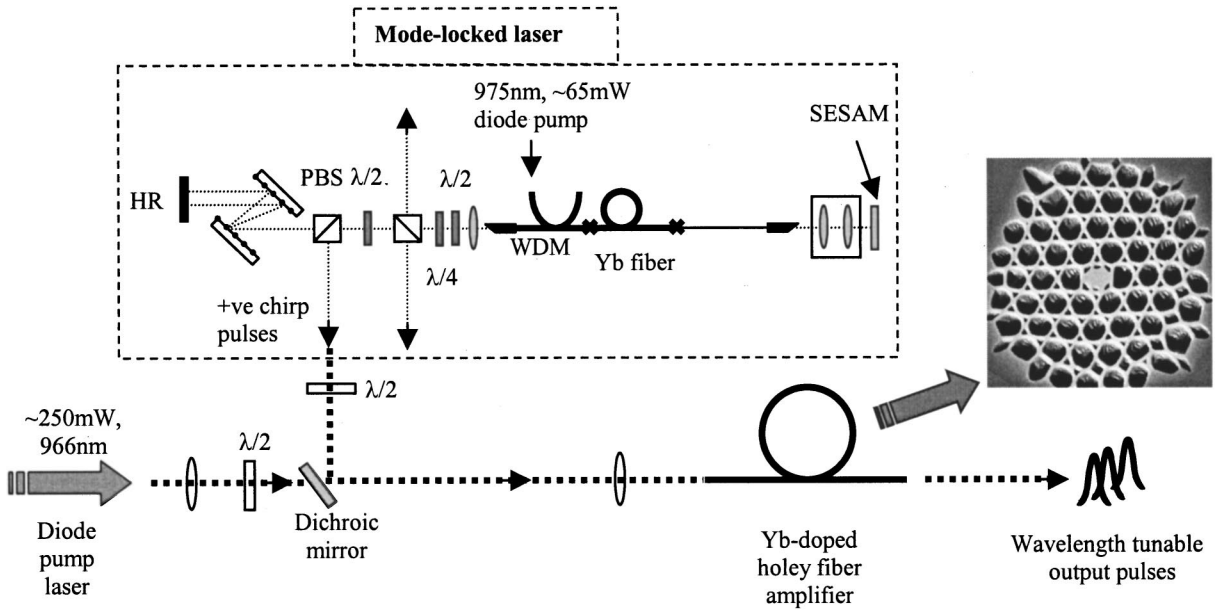

Fig. 1. Experimental setup, showing the in-house mode-locked Yb^{3+} fiber seed laser (diode pumped), the launch arrangement for seeding the pulses and the pump laser to the Yb^{3+} doped holey fiber amplifier, and an inset SEM of the holey fiber structure. HR, high-reflectivity mirror; +ve, positive, WDM, wavelength-division multiplexer; PBS, polarizing beam splitter.

In this section we describe in greater detail the system's operating principles and experimental setup and the theoretically calculated properties of the holey fiber. Subsection 2.A describes the operating principles of the system, and then Subsection 2.B provides details of the seed oscillator's performance and the arrangement for launching seed pulses and cw pump power into the amplifier. Subsection 2.C explains the holey fiber's characteristics.

A. Operating Principles

Here we describe in greater detail the processes that govern the pulse evolution within the amplifier. It should be appreciated that there is a complicated interplay among gain, dispersion, and nonlinear interactions. A schematic illustration of the key features of the pulse evolution, both in the spectral domain and in the time domain, is shown in Fig. 2.

The pulses at the amplifier input have a positive linear chirp and a peak power substantially below that required for soliton formation. In our experiments the pulses have a duration of 2.4 ps, a peak power of ~5 W, and a chirp of ~0.15 ps/nm and can be compressed to ~110 fs by use of a grating pair. Figure 2 shows that, in the time domain, the pulse duration initially decreases owing to linear pulse compression over the first few tens of centimeters of the amplifier because the holey fiber has anomalous dispersion (~100 ps nm^{-1} km^{-1}); which compensates for the initial positive chirp. At this stage there is no nonlinear distortion of the initial, smooth spectrum. Then, as the pulse is progressively amplified and compressed, the peak power rapidly increases and soon exceeds the threshold for nonlinear interactions and the formation of a fundamental, and then (possibly) a higher-order, soliton. The higher-order soliton pulse evolution is manifested in the temporal domain where the pulse undergoes soliton compression, so further increasing the peak power and accelerating the nonlinear pulse evolution.

The effects of intrapulse stimulated Raman scattering transfer the energy from the high-frequency part of the pulse spectrum to the low-frequency part. This destabilizes the pulse and ultimately results in breakup of the pulse into a peak and pedestal and, most importantly, in the formation of a Raman soliton. The Raman soliton pulse is a stable entity, which because of the SSFS effect continuously downshifts its central frequency (moves to longer wavelengths) as it moves along the amplifier. It should be noted that the SSFS process is strongly dependent on the pulse duration as the rate of frequency shift is proportional to $\Delta\tau^{-4}$, where $\Delta\tau$ is the FWHM of the pulse.

The final wavelength of the solitons at the amplifier output is sensitive to the amplifier gain settings, i.e., gain distribution, pump power, and amplifier length. The gain window of the Yb^{3+}-doped amplifier extends from 1.03 to 1.12 μm, so the wavelength-shifting soliton will experience further gain after formation until either the amplifier gain is saturated or the pulse wavelength is redshifted beyond the gain window. Once the SSFS has shifted the wavelength of the pulses beyond the ~1.12-μm upper limit of the amplifier gain spectrum, the soliton will neither be amplified nor suffer absorption

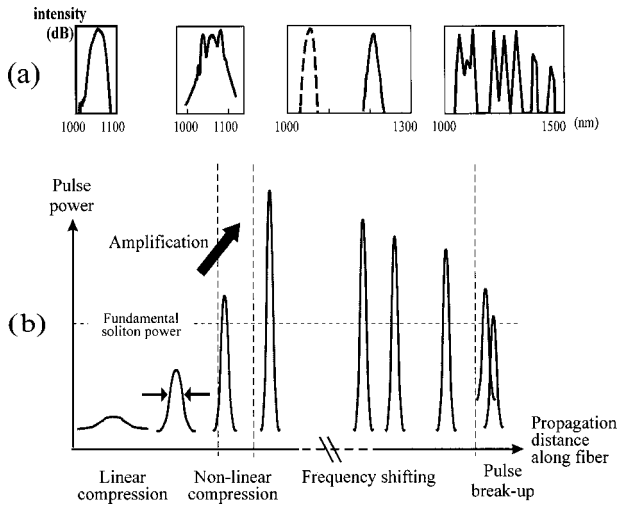

Fig. 2. Representation of the pulse evolution with propagation distance along the holey fiber amplifier: (a) frequency domain, optical spectra; (b) time domain, pulse duration/peak power.

caused by Yb^{3+}-doping and will propagate as if it were in a passive holey fiber. However, the Yb^{3+}-doped core will continue to act only on the non-Stokes-shifted pedestal of the initial pulse that is left after the Raman soliton has been generated. Use of an overlong amplifier will cause the excess (unpumped) length to act as an absorber for residual unshifted radiation at the seed wavelengths, whereas the SSFS redshifted components that fall outside the Yb^{3+} absorption band will pass with minimal attenuation, leaving a spectrally filtered, wavelength-shifted Raman soliton at the system output.

The maximum wavelength shift of the Raman soliton increases steadily with the length of fiber used, so the maximum obtainable wavelength will, in principle, have an upper bound set by the absorption of silica near 2.3 μm.[5] Other factors, such as the variation of the fiber dispersion over the wavelength range of interest, may limit the maximum obtainable wavelength in practice.

Finally, it is worth noting that, depending on the seed pulse energies, amplifier length, and pump power, it is possible to enter a more-complicated regime of pulse evolution in which the pulse breaks up into multicolored solitons at the amplifier output. In our experiments we managed to form pulse bursts with as many as six individual multicolored pulses, and in some instances wavelengths approaching 1.58 μm were observed. Here the seed pulse (or a previously formed Raman soliton) breaks up into several Raman solitons, each of which will have somewhat different characteristics at the point of formation and will evolve separately with further propagation. A burst of multicolored solitons is thus observed at the end of the amplifier.

For simplicity, in the above discussion we considered only the case of a forward-pumped amplifier and positively chirped seed pulses, as this was the configuration that we studied in the greatest detail experimentally and that gave the best tuning characteristics. We note that in other configurations, e.g., a forward-pumped amplifier with close to transform-limited seed pulses, the general features of the pulse formation processes would not change dramatically.

Whereas the description given above is purely qualitative, it should be noted that detailed models have been applied numerically to describe Raman soliton formation in fiber amplifiers. For example, an approach based on a modified nonlinear Schrödinger equation, which incorporated terms to describe a gain medium with a Lorentzian line shape and allowing for the effects of gain saturation along the amplifier length, was reported previously.[15] This model treats stimulated Raman scattering by using an optically driven molecular vibration model. The model has been used to simulate the amplification of ~500-fs pulses in an erbium-doped fiber amplifier, and good quantitative agreement between the experimental and theoretical data was obtained. Others[16] have performed simulations of the propagation of pulses with widths approximately equal to the inverse bandwidth of the amplifier and suggest that the Maxwell–Bloch equations are necessary if an accurate quantitative analysis of the system is required. These theoretical approaches, with the inclusion of appropriate gain spectrum as a function of amplifier length, could readily be adapted to model our experiments in holey fiber, although we have not done this at the time of writing.

B. System Implementation

Our experimental set up is shown in Fig. 1. The two principal components are a mode-locked seed laser emitting ultrashort pulses at 1.06 μm and an anomalously dispersive Yb^{3+}-doped holey fiber amplifier.

We used an in-house Yb^{3+}-doped, stretched pulse mode-locked fiber laser source as our master oscillator.[17] It represents a far more practical and stable source than the short-pulse Yb^{3+} silica fiber oscillator first demonstrated in 1997.[18] Mode-locked operation is based on the stretched pulse principle,[19] which employs nonlinear polarization rotation within the fiber as a fast saturable absorber.[20] The cavity has a Fabry–Perot geometry and incorporates a semiconductor saturable-absorber mirror (SESAM; Fig. 1) to facilitate reliable self-start mode locking. By suitable selection of the output port from the laser, positively chirped, ~2.4-ps-duration Gaussian pulses (compressible to 108 fs with an external-cavity diffraction grating pair) could be obtained at the output. The second-harmonic (SHG) autocorrelation trace and the spectrum of the pulses incident to the holey fiber amplifier are shown in Figs. 3(a) and 3(b), respectively. Note that the smooth spectrum over the wide dynamic range of the measurement instrument facilitates observation of nonlinear spectral distortion. The average laser output power was ~3 mW at a pulse repetition rate of 54 MHz (~60-pJ pulse energy). The laser output is exceptionally stable, and we measured the amplitude noise to be ~0.05%. The laser therefore represents an attractive and practical seed for Raman soliton experiments, which are naturally highly sensitive to amplitude noise.

The positively chirped pulses from our oscillator were launched into a length of Yb^{3+}-doped holey fiber amplifier, which for the majority of experiments undertaken was codirectionally pumped by a 966-nm diode based master oscillator power amplifier (maximum output power, ~250 mW). We achieved approximately 20% coupling efficiency into the holey fiber for both the seed pulses and the pump radiation, giving a maximum launched pulse energy of ~10 pJ and as much as 50 mW of launched pump. We used a half-wave plate to match the laser output polarization to a principal axis of the highly birefringent Yb^{3+}-doped holey fiber. We note that our results were insensitive to the orientation of the 966-nm diode pump polarization relative to the fiber polarization axes. The pulses emerging from the output end of the amplifier were characterized in the frequency domain by use of an optical spectrum analyzer and in the time domain by a noncollinear, second-harmonic intensity autocorrelator with ~10-fs resolution. For our experiments the holey fiber amplifier had a length of 1.7–9 m.

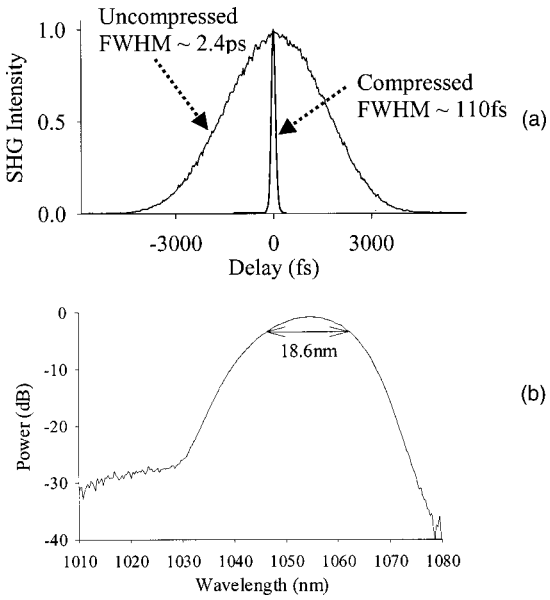

Fig. 3. Seed pulses from a mode-locked laser: (a) Autocorrelation of chirped seed pulses and of unchiped pulses ($\Delta\nu\Delta\tau \sim 0.55$) compressed by use of a diffraction grating pair; (b) pulse spectrum.

C. Characteristics of the Yb^{3+}-Doped Holey Fiber

A scanning-electron micrograph (SEM) of the transverse cross section of the Yb^{3+}-doped holey fiber used in these experiments is shown in the inset of Fig. 1. The holey cladding region was fabricated by standard capillary stacking techniques,[21] and an Yb^{3+}-doped solid rod was used to form the core. The core of this fiber is approximately 2 μm in diameter, and the surrounding cladding is composed largely of air. These factors combine to result in tight confinement of the guided mode to the fiber core. Hence the fiber has an extremely high effective nonlinearity coefficient, $\gamma = n_2/A_{\text{eff}}$, where n_2 is the intrinsic material nonlinearity and A_{eff} is the effective mode area.[13] This high nonlinearity allows short device lengths to be used for the SSFS. Note that this fiber is observed to be strictly single mode for all wavelengths considered here (including the 966-nm pump wavelength).

Yb^{3+} ions are incorporated across the central 1.7 μm of the core to a concentration of 2000–3000 parts in 10^6, as estimated from white-light measurements of fibers drawn from the unetched Yb^{3+}-doped fiber preform used to fabricate the core rod. The holey fiber used in the present

experiment was recently used to make what to our knowledge was the first demonstration of a mode-locked holey fiber laser,[22] and a slope efficiency of >60% was achieved.

To predict the dispersion properties and the mode field diameter of the doped holey fiber shown in Fig. 1 we used a numerical technique described previously.[8,23] This approach is a hybrid modal method, in which the complex transverse refractive-index structure is described by a Fourier decomposition, and the guided mode(s) by localized Hermite–Gaussian functions. For the purposes of predicting the properties of the fiber in Fig. 1, we used the actual SEM of the fiber's transverse profile to define the refractive-index distribution in the numerical model. In this way the influence of any distortions or irregularities in the otherwise periodic structure could be accounted for in the resulting predictions. Because of the large air fill fraction it is necessary to use a full vector model to make accurate predictions, and both even and odd terms have been used in the modal expansions (as in Ref. 24) to ensure that any asymmetries in the fiber profile can also be modeled accurately. Note that the material dispersion of silica was included explicitly in these calculations.

As a consequence of the combination of core asymmetry, high refractive-index contrast, and the small scale of the structure, this fiber is extremely birefringent (strongly polarization maintaining). In Fig. 4 we plot the transmission characteristics of polarized broadband light at 1540 nm through crossed polarizers and 1.2 m of the fiber. From a measurement of the spectral period of the transmission we estimate a birefringent beat length of just 0.3 mm at 1.54 μm. This value agrees well with our prediction of 0.27 mm from the model described above. As far as we are aware, this is one of the shortest beat lengths ever obtained for an optical fiber.

The model's predictions for the mode area (A_{eff}) and dispersion (D) as a function of wavelength are shown in Fig. 5. To demonstrate the effect of the fiber asymmetry we have shown results for both polarization axes. Unsurprisingly, A_{eff} does not differ greatly on the separate polarization axes. A_{eff} is $\sim$2.5 μm^2 at a wavelength of 1.55 μm, which is approximately 30 times smaller than for a standard single-mode fiber (e.g., Corning SMF28). We also note that A_{eff} increases with increasing wavelength, indicating that the mode is more tightly confined to the fiber core at shorter wavelengths. To give an indication of its exceptional nonlinear properties, we note that, for a 200-fs (FWHM) pulse (1.06-μm wavelength) propagating within this fiber, the fundamental soliton power and soliton period are approximately 50 W and 60 cm, respectively. As mentioned above, these values are significantly lower than the comparable values for experiments performed in standard fiber ($\lambda \sim 1.5$ μm) by other authors. The dispersion properties of the two axes are markedly different, which indicates that the dispersion is much more sensitive to the hole arrangement then is A_{eff}. The zero-dispersion wavelengths [above which the dispersion is anomalous (positive)] for the separate polarization axes are at 770 and 830 nm, respectively, and at a wavelength of 1.06 μm the dispersion on the two axes differs by $\sim$35 ps/(nm/km). The relatively flat dispersion curves, particularly in the 1.0–1.3-μm wavelength range and combined with the high effective nonlinearity of the fiber, facilitate good wavelength tuning through the SSFS effect.

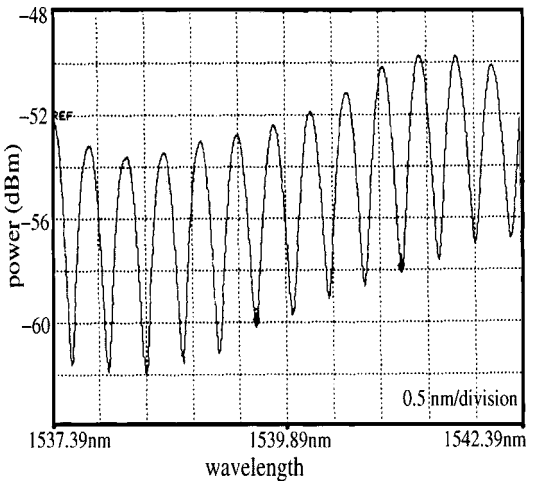

Fig. 4. Transmission spectrum (after a polarization beam splitter) showing the high birefringence of this elliptical core holey fiber (1.2-m length).

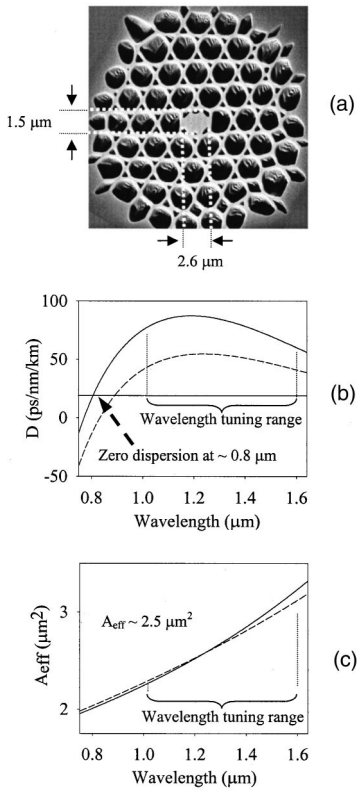

Fig. 5. Characteristics of the Yb^{3+}-doped holey fiber. (a) SEM of the structure, showing the dimensions of the elliptical core. (The metallic coating required for producing SEM images enlarges the fine silica bridges by $\sim$50 nm, which is taken into account when we calculate the fiber characteristics.) (b) Dispersion predictions for the two principal polarization axes. (c) Effective mode area (A_{eff}) predictions for the two principal polarization axes.

3. RESULTS AND DISCUSSION

The output characteristics of our system were of three distinct types. Perhaps the most useful from a practical

perspective is the single-color, wavelength tunable soliton regime. Here we obtained high-quality pulses at a distinct wavelength tunable from 1.06 to 1.33 μm, with the wavelength controlled by varying the pump power of the amplifier. We could also obtain more-complex spectral output, which we characterized as multicolor solitons and also broadband continuous spectra. These spectra were observed when we used seed pulses with ~25% higher energy (the oscillator has a variable output coupling) than for the single-color soliton regime, and (generally) at the highest pump powers. Finally, by using a shorter-length amplifier and reducing the chirp of the seed pulses we could avoid the pulse breakup and wavelength-shifting effects and observe temporal compression of the seed pulses. We describe each regime of operation in greater detail below.

A. Single-Color, Wavelength Tunable Solitons

We found that forward pumping an approximately 4-m length of holey fiber amplifier was the optimal configuration for producing single-color, wavelength tunable solitons. In particular, we used a 4.7-m length of amplifier fiber and measured the output spectra and autocorrelations of the pulses emerging from the amplifier as a function of pump power. In Fig. 6(a) we show the superposed spectra of the pulse emerging from the amplifier as the incident pump power delivered to the amplifier is increased. As can be seen from Fig. 6(a), a single, spectrally distinct Raman soliton of ~20-nm bandwidth is generated at the system output for pump powers above the minimum threshold power required for appreciable SSFS effects (>50-mW incident pump power) to be obtained. As the pump power is increased, the final wavelength of the pulses progressively increases. Residual radiation at the original seed wavelength of ~1056 nm remains in each instance. The dependence of the final pulse wavelength on the amplifier pump power is shown in Fig. 6(b). The final central wavelength of the pulses is seen to vary in an almost linear fashion with the level of incident pump power.

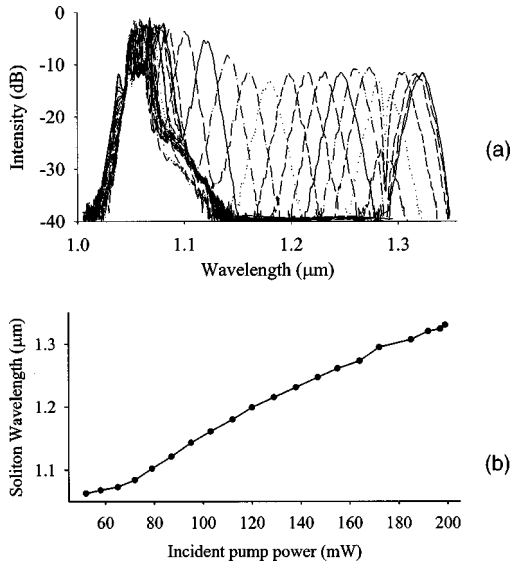

Fig. 6. Tunable single-color solitons: (a) superimposed spectra of the solitons shifted to progressively longer wavelengths (1.06–1.33 μm), (b) plot of the soliton wavelength versus amplifier (incident) pump power.

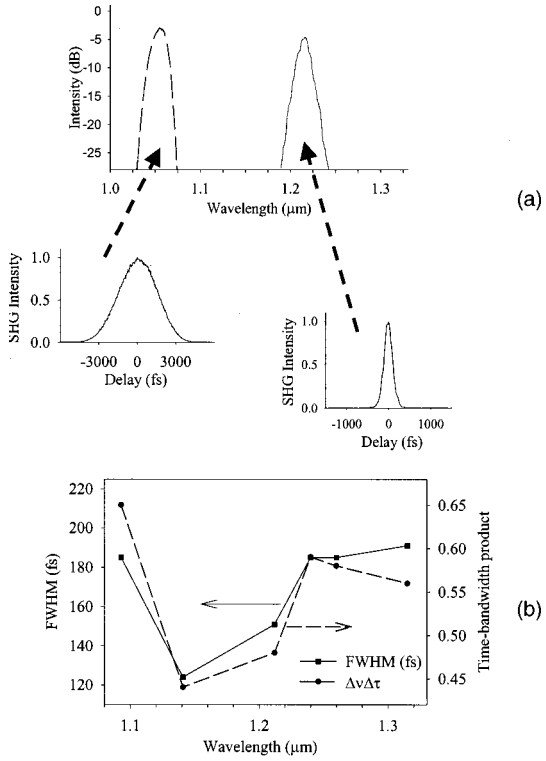

Fig. 7. Autocorrelation measurements of the wavelength-shifted solitons. (a) Spectrum and corresponding autocorrelation traces for the seed pulse for a wavelength-shifted pulse at 1.24 μm. (b) Plot of pulse duration and time–bandwidth product versus soliton pulse wavelength.

We attribute the increase in soliton wavelength with pump power to the fact that at higher pump powers the resultant change in gain distribution causes the Raman solitons to form earlier within the amplifier, thereby leaving them a greater length of fiber within which to walk off to longer wavelengths through SSFS. The roll-off in peak spectral intensity with increased pump power observed in Fig. 6(a) is consistent with this explanation, as the earlier the pulses get shifted out of the amplifier gain bandwidth, the lower the overall amplification experienced by the pulse and the greater the redshift.

We also performed the pulse autocorrelation measurements for pulses at various output wavelengths (amplifier pump powers) to establish how the pulse quality varied across the tuning range. The results of these measurements are shown in Fig. 7. To illustrate the typical pulse quality we show in Fig. 7(a) the autocorrelation function and spectrum at a wavelength of 1240 nm. The pulse duration in this instance was 150 fs, and the time–bandwidth product 0.48. The measurements plotted in Fig. 7(b) show that the pulse duration remains approximately constant, ~180 fs FWHM, as the wavelength is tuned and that the pulse quality as defined by the time–bandwidth product remains high across the full tuning range.

Finally, we investigated the effect of reversing the amplifier pump direction. Using the 2.4-ps, linearly chirped pulses directly from the mode-locked laser as a seed for a

1.7-m length of amplifier fiber, we obtained a similar SSFS tuning curve but obtained a maximum wavelength shift to only 1.12 μm. The wavelength tuning range was therefore much narrower than that achieved for the forward-pumped amplifier. The reduction in wavelength tuning range is understandable because in this backward-pumping configuration any unbleached length of Yb^{3+}-doped fiber at the front of the amplifier absorbs the signal, thereby frustrating soliton formation early within the fiber. The effective length of fiber available for wavelength shifting through the SSFS is therefore less than in the forward-pumping configuration.

Note that, because of the practical difficulties of working with such small-core fibers compounded by the issue of pulse breakup and wavelength shift within the amplifier, it was not possible for us to quantify the precise gain experienced by a given pulse for a given pump power and amplifier configuration. All that we are really able to say is that the maximum overall single-pass gain through the system was greater than ~17 dB. This estimate takes into account the amplifier setup used in the experiments, i.e., a flat cleaved facet at the input (to maximize the launched signal), which would provide 4% feedback, and an angle cleaved facet (reducing feedback to <1%) at the exit end of the amplifier. In every amplifier configuration we were able to increase the pump power sufficiently to obtain laser operation (at some wavelength within the Yb^{3+} bandwidth) from the system; so for the end reflections, as stated above, at least a 17-dB gain is achieved.

B. Multicolor Solitons and Broadband Continuous Spectra

It did not prove possible for us to extend the single-pulse tuning range beyond 1.33 μm. Instead, when we maximized the output power of our seed oscillator to increase the launched pulse energy to ~12 pJ (compared to ~9 pJ for the single-color soliton experiments), we observed the generation of multicolor pulses (separated in wavelength and time), which increased in number as we increased the pump power, as shown in Fig. 8. Using a longer (9-m) length of amplifier fiber and operating at the highest pump powers, we observed more-complex spectra, including increased numbers of multicolor solitons, and a broadband continuous (time-averaged) optical spectrum, which was similar to that achieved in supercontinuum generation experiments in passive holey fiber.[6] Figure 9(a) shows that for the most complex multicolor soliton spectra a far greater maximum wavelength shift, as much as 1.58 μm, could be seen (the peak was measured with the maximum redshift). A typical example of a broadband continuous spectrum is shown in Fig. 9(b) with wavelengths extending from 1.03 to 1.62 μm. This broad spectrum could be useful for applications such as optical coherence tomography. At present this mode of operation is not fully understood.

C. Temporal Compression

We also investigated the conditions required for temporal compression of the input pulses (through multisoliton effects) as a function of amplifier pump power. By changing both the chirp of the input pulses and the length of the amplifier fiber we investigated the optimum conditions for pulse compression. We optimized the chirp of the input pulses by extracting negatively chirped pulses from the oscillator (previously we had selected the output port for positively chirped pulses) and transforming these pulses to have a small positive chirp by propagation through a length of standard fiber. We performed cutback measurements to obtain pulses of the desired dura-

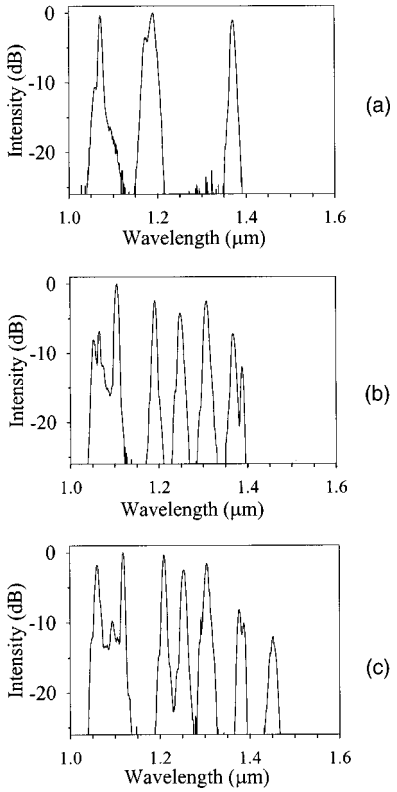

Fig. 8. Multicolor solitons, showing increasingly complex spectra as the amplifier pump power is increased.

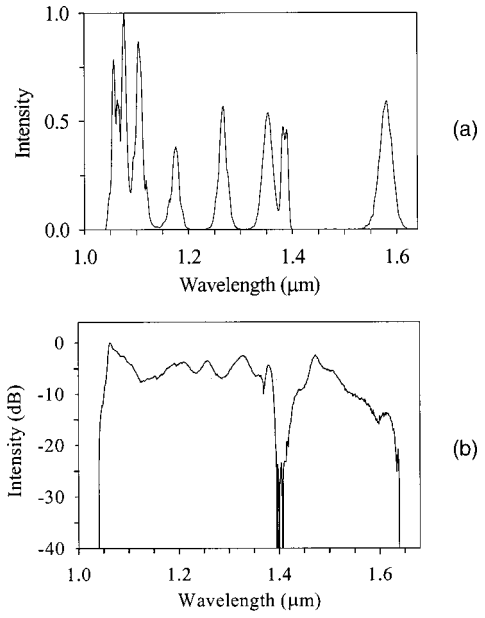

Fig. 9. (a) Typical example of complex multicolored soliton spectra extending to $\lambda \sim 1.58$ μm. (b) Broadband continuous spectrum extending to $\lambda \sim 1.62$ μm.

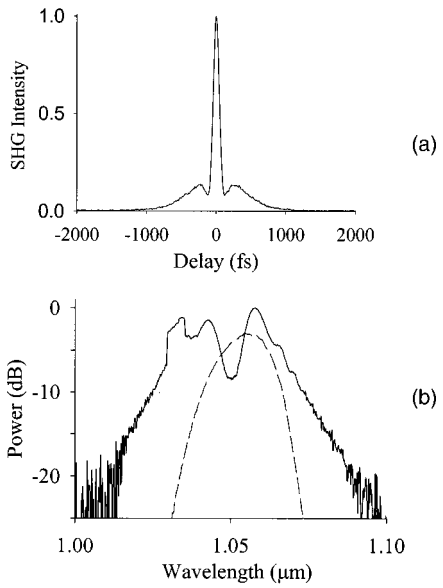

Fig. 10. Temporally compressed pulses: (a) autocorrelation trace ($\tau \sim 67$ fs), (b) spectra of a seed pulse (dashed curve) and a compressed pulse (solid curve).

tion and hence chirp. In a similar fashion we optimized the amplifier length with respect to the minimum pulse duration at the amplifier output by measuring the output pulse's duration in a series of cutback measurements of the amplifier fiber. By launching the optimally chirped (~0.02-ps/nm) pulses into a 2.8-m-long holey fiber amplifier we obtained pulses compressed to 67 fs FWHM. The autocorrelation and the spectra of the compressed pulses are shown in Figs. 10(a) and 10(b), respectively. Although we expect the soliton formation process in this case to be broadly similar to that described above, because the chirp of the input pulses is smaller it is more rapidly compensated for (by the anomalous dispersion of the holey fiber) in a shorter length of amplifier fiber. Breakup into multiple solitons is prevented because the pulses exit the amplifier before they evolve beyond the temporally compressed state.

4. CONCLUSIONS

In conclusion, we have developed a continuously tunable soliton source based on diode-pumped active microstructured holey fiber seeded by pulses from a femtosecond, mode-locked fiber source. We control the tuning of the output wavelength by changing the amplifier pump power. Discrete single-color solitons have been demonstrated to be of high quality ($\Delta\nu\Delta\tau \sim 0.55$), and the central wavelength has been shown to be tunable across the range 1.06–1.33 μm. Multicolored solitons were demonstrated at wavelengths up to 1.58 μm, and continuous spectra were demonstrated that span 1.03–1.62 μm. We demonstrated temporal compression of the pulses to 67 fs (FWHM) compared with the minimum pulse duration of 110 fs obtainable with linear dispersion compensation of pulses directly from our oscillator (by use of a diffraction grating pair).

We have modeled the dispersion properties of the holey fiber by using the exact fiber structure (recorded using SEMs), and we have presented a brief overview of the relevant physical processes on which the system is based. Note that our present results combined with previously reported results from SSFS systems mean that it is now possible to generate femtosecond pulses at any wavelength from 1 to 2.2 μm by use of fiber-based techniques. Furthermore, it likely that with detailed quantitative modeling and optimization of our present system it may well be possible to develop this single source to give SSFS wavelength tunable output anywhere in the range from 1 to 2 μm. We believe this to be an exciting development of fiber technology, providing a device with great potential for widespread practical applications.

ACKNOWLEDGMENTS

J. H. V. Price acknowledges the support provided by the Engineering and Physical Sciences Research Council, (EPSRC), UK, during the course of this research. T. M. Monro and D. J. Richardson are supported by the Royal Society through the University Research Fellowship Scheme. This research was supported by EPSRC research grant GR/N10820. The development of the mode-locked, Yb^{3+}-doped fiber oscillator was supported by Positive Light, Inc. (USA) and the research group based at ETH, Zurich, led by U. Keller.

D. J. Richardson's e-mail address is djr @orc.soton.ac.uk.

REFERENCES

1. F. M. Mitschke and L. F. Mollenauer, "Discovery of the soliton self-frequency shift," Opt. Lett. **11**, 659–661 (1986).
2. J. P. Gordon, "Theory of the soliton self-frequency shift," Opt. Lett. **11**, 662–664 (1986).
3. E. M. Dianov, A. Y. Karasik, P. V. Mamyshev, A. M. Prokhorov, V. N. Serkin, M. F. Stel'makh, and A. A. Fomichev, "Stimulated-Raman conversion of multisoliton pulses in quartz optical fibers," JETP Lett. **41**, 294–297 (1985).
4. N. Nishizawa and T. Goto, "Compact system of wavelength-tunable femtosecond soliton pulse generation using optical fibers," IEEE Photon. Technol. Lett. **11**, 325–327 (1999).
5. M. E. Fermann, A. Galvanauskas, M. L. Stock, K. K. Wong, D. Harter, and L. Goldberg, "Ultrawide tunable Er soliton fiber laser amplified in Yb-doped fiber," Opt. Lett. **24**, 1428–1430 (1999).
6. J. K. Ranka, R. S. Windeler, and A. J. Stentz, "Visible continuum generation in air-silica microstructure optical fibers with anomalous dispersion at 800 nm," Opt. Lett. **25**, 25–27 (2000).
7. T. A. Birks, W. J. Wadsworth, and P. St. J. Russell, "Supercontinuum generation in tapered fibers," Opt. Lett. **25**, 1415–1417 (2000).
8. T. M. Monro, D. J. Richardson, N. G. R. Broderick, and P. J. Bennett, "Holey optical fibers: an efficient modal model," J. Lightwave Technol. **17**, 1093–1102 (1999).
9. T. A. Birks, D. Mogilevtsev, J. C. Knight, and P. St. J. Russell, "Dispersion compensation using single-material fibers," IEEE Photon. Technol. Lett. **11**, 674–676 (1999).
10. X. Liu, C. Xu, W. H. Knox, J. K. Chandalia, B. J. Eggleton, S. G. Kosinski, and R. S. Windeler, "Soliton self-frequency shift in a short tapered air-silica microstructure fiber," Opt. Lett. **26**, 358–360 (2001).
11. J. H. Price, W. Belardi, L. Lefort, T. M. Monro, and D. J. Richardson, "Nonlinear pulse compression, dispersion com-

pensation, and soliton propagation in holey fiber at 1 micron," in *Nonlinear Guided Waves and Their Applications*, Vol. 55 of OSA trends in Optics and Technology Series (Optical Society of America, Washington, D.C., 2001), paper WB1-2.
12. W. J. Wadsworth, J. C. Knight, A. Ortigosa-Blanch, J. Arriaga, E. Silvestre, and P. St. J. Russell, "Soliton effects in photonic crystal fibres at 850 nm," Electron. Lett. **36**, 53–55 (2000).
13. G. P. Agrawal, *Nonlinear Fiber Optics*, 2nd ed. (Academic, San Diego, Calif., 1995).
14. R. Holzwarth, T. Udem, T. W. Hänsch, J. C. Knight, W. J. Wadsworth, and P. St. J. Russell, "Optical frequency synthesizer for precision spectroscopy," Phys. Rev. Lett. **85**, 2264–2267 (2000).
15. D. J. Richardson, V. V. Afanasjev, A. B. Grudinin, and D. N. Payne, "Amplification of femtosecond pulses in a passive, all-fiber soliton source," Opt. Lett. **17**, 1596–1598 (1992).
16. J. T. Manassah and B. Gross, "Propagation of femtosecond pulses in a fiber amplifier," Opt. Commun. **122**, 71–82 (1995).
17. J. H. Price, L. Lefort, D. J. Richardson, G. J. Spuhler, R. Paschotta, U. Keller, C. Barty, A. Fry, and J. Weston, "A practical, low noise, stretched pulse Yb^{3+} doped fiber laser," in *Conference on Lasers and Electro-Optics (CLEO)*, Vol. 56 of OSA Trends in Optics and Photonics Series (Optical Society of America, Washington, D.C., 2001), paper CTuQ6.
18. V. Cautaerts, D. J. Richardson, R. Paschotta, and D. C. Hanna, "Stretched pulse Yb^{3+}: silica fiber laser," Opt. Lett. **22**, 316–318 (1997).
19. K. Tamura, E. P. Ippen, H. A. Haus, and L. E. Nelson, "77-Fs pulse generation from a stretched-pulse mode-locked all-fiber ring laser," Opt. Lett. **18**, 1080–1082 (1993).
20. M. H. Ober, M. Hofer, U. Keller, and T. H. Chiu, "Self-starting diode-pumped femtosecond Nd fiber laser," Opt. Lett. **18**, 1532–1534 (1993).
21. P. J. Bennett, T. M. Monro, and D. J. Richardson, "Toward practical holey fiber technology: fabrication, splicing, modeling, and characterization," Opt. Lett. **24**, 1203–1205 (1999).
22. K. Furusawa, T. M. Monro, P. Petropoulos, and D. J. Richardson, "Modelocked laser based on ytterbium doped holey fibre," Electron. Lett. **37**, 560–561 (2001).
23. T. M. Monro, D. J. Richardson, N. G. R. Broderick, and P. J. Bennett, "Modeling large air fraction holey optical fibers," J. Lightwave Technol. **18**, 50–56 (2000).
24. T. M. Monro, N. G. Broderick, and D. J. Richardson, "Exploring the optical properties of holey fibers," in *Nanoscale Linear and Nonlinear Optics: International School on Quantum Electronics, Erice, Sicily, July 2000* AIP Conf. Proc. **560**, 123–128 (2001).